Coordination variation of hydrated Cu2+/Br1− ions traversing the interfacial water in mesopores

Q. Wang, X. F. Huang, C. X. Li, L. Q. Pan, Z. H. Wu et al.

Citation: AIP Advances **2**, 022107 (2012); doi: 10.1063/1.4704545

View online: http://dx.doi.org/10.1063/1.4704545

View Table of Contents: http://aipadvances.aip.org/resource/1/AAIDBI/v2/i2

Published by the American Institute of Physics.

Coordination variation of hydrated Cu^{2+}/Br^{1-} ions traversing the interfacial water in mesopores

Q. Wang,[1] X. F. Huang,[1,2] C. X. Li,[1] L. Q. Pan,[2] Z. H. Wu,[3] T. D. Hu,[3] Z. Jiang,[4] Y. Y. Huang,[4] Z. X. Cao,[1,a] G. Sun,[1] and K. Q. Lu[1]
[1]*Institute of Physics, Chinese Academy of Sciences, Beijing 100190, China*
[2]*Department of Physics, University of Science and Technology Beijing, Beijing 100083, China*
[3]*Institute of High Energy Physics, Chinese Academy of Sciences, Beijing 100039, China*
[4]*Shanghai Institute of Applied Physics, Chinese Academy of Sciences, Shanghai 201204, China*

(Received 27 February 2012; accepted 28 March 2012; published online 11 April 2012)

Resolution of the atomistic and electronic details about the coordination structure variation of hydrated ions in the interfacial water is still a tough challenge, which is, however, essentially important for the understanding of ion adsorption, permeation and other similar processes in aqueous solutions. Here we report the tracing of coordination structure variation for hydrated Cu^{2+}/Br^{1-} ions traversing the interfacial water in Vycor mesopores ($\phi = 7.6$ nm) by employing both X-ray absorption near edge structure and extended X-ray absorption fine structure spectroscopies. By controlled desorption/adsorption of water, the filling fraction of the mesopores, thus the water layer thickness, can be adjusted, which in turn effects the variation of coordination structure of the ions therein. It is found that both Cu^{2+} and Br^{1-} ions prefer staying exclusively in the core water, and in this circumstance no ion pairs have been detected in the solution of concentrations up to 1.0 M. Following capillary decondensation occurring at a filling fraction of ~35% which corresponds to a water layer of about three monolayers, Br^{1-} ions begin immediately to reconstruct their first coordination shell, characterized by ionic dehydration, shrinkage of ion-water bond length, and formation of ion pairs. In contrast, Cu^{2+} ions can retain a bulk-like coordination structure till being driven to bond directly to the pore surface when the filling fraction is below 20%. At the final stage of dehydration via thermal vacuum treatment at 110°C, Cu^{2+} ions can be completely reduced to the Cu^{1+} state, and recover at room temperature only when the filling fraction is above 14%. These results may be inspirable for the investigation of similar problems concerning hydrated ions in water solution under different confining conditions. [http://dx.doi.org/10.1063/1.4704545]

I. INTRODUCTION

The coordination structure of hydrated ions is usually very sensitive to the condition of the surrounding water. When a hydrated ion goes from bulk-like water of a high dielectric constant into a region of low dielectric constant, e.g., interfacial water confined in nanopores or in bio-channels, its self-energy increases.[1] This self-energy increase constitutes the main barrier for ion transportation through the nanometer-thick interfacial water involved in ion adsorption and in selective ion permeation driven by, say, electrostatic interaction between the ion and the charged solid surface.[2,3] The atomistic mechanism of this energy barrier has been attributed to ionic dehydration without providing any further details such as how a hydrated ion adjusts its coordination structure.[4] Reliable experimental data concerning how the interfacial or confinement condition of water alters the

[a]To whom correspondence should be addressed. E-mail: zxcao@iphy.ac.cn

coordination structure of hydrated ions are extremely rare, let alone the isolation of the effect of interfacial water from that of confined water.[5]

The inner-sphere and outer-sphere surface complexation for adsorbed ions at the metal oxide-aqueous solution interface has been extensively discussed.[6] For the inner-sphere complex no water molecules are available between the adsorbed ions and the solid surface, whereas in the outer-sphere complex one or more water molecules may be incorporated. At the mica-aqueous solution interface, with pH = 5.5 for the solution, it was experimentally confirmed that Rb^+ ions form outer-sphere complexes, whereas for Sr^{2+} ions inner-sphere complexes ensue.[7] At above pH_{pzc}, the pH value at the point of zero charge, cations such as Na^+, Rb^+, Ca^{2+}, Sr^{2+}, Zn^{2+}, Y^{3+} and Nd^{3+} are found forming inner-sphere complexes, bonding directly to the oxygen atoms at the rutile surface.[2,6,8,9] The adsorption of some transition metal ions and also ions of Pb on hydroxide surfaces was also discussed.[2,8,9] It should be pointed out that all the works mentioned above are mainly concerned with the final status of ionic adsorption, referring to the surface complexation modes and the distribution of ions within the interfacial water. A dynamic picture for the formation and variation of the complexes is still missing.

Ionic adsorption from an aqueous solution is determined by the energy cost for a hydrated ion to arrive at the surface, as well as by the electrostatic interaction between the ion and the charged surface. In the investigations carried out up to now, the probed signals usually come from both the ions adsorbed on the surface and the ions in the interfacial water.[2,6–9] Consequently, the impact of interfacial water alone on the coordination structure of the hydrated ions is still unknown, which is, however, essentially important for the understanding of ionic adsorption and permeation. It is utterly desirable to prepare a scenario where initially the hydrated ions stay only in the interfacial water.

X-ray absorption spectroscopy (XAS) is an effective tool to trace the local, dynamic structure change of hydrated ions in the interfacial water layer.[2,9,10] Cu^{2+} and Br^{1-} ions are very favorable for such research because they are very suitable for XAS analysis. In addition, the coordination structure of Cu^{2+} and Br^{1-} ions in bulk solution of different concentrations has been widely investigated, both experimentally and by simulation, and those results can serve as a good reference.[11–18] Moreover, a nearly-neutral mesopore surface suffices to prevent direct bonding of these ions to the surface, consequently a scenario with all the ions initially staying in the interfacial water can be realized. For Vycor glass, pH_{pzc} ~2.0, and no obvious adsorption of Cu^{2+} ions onto the Vycor surface occurs if the pH value of the solution is below 4.0.[6] If the research is to be carried out on the 0.1 M $CuBr_2$ aqueous solution, of which pH = 4.0, loaded in Vycor mesopores, the disturbing effect of surface charge on the hydrated ions can be excluded since in the more concentrated solutions resulting from water desorption, the pH value maintains below 4.0. Thus the 0.1 M $CuBr_2$ aqueous solution loaded in Vycor mesopores can be an ideal system for the study of impact of interfacial water on the coordination structure of hydrated ions by XAS analysis.

In this work, by using XAS analysis including both X-ray absorption near edge structure (XANES) and extended X-ray absorption fine structure (EXAFS) spectroscopic measurements, we successfully traced the dynamic coordination structure variation of hydrated Cu^{2+}- and Br^{1-} ions in the desorption-adsorption cycle performed on 0.1 M $CuBr_2$ aqueous solution loaded in Vycor mesopores. It is found that following decondensation, the Br^{1-} ions start immediately to reconstruct their coordination shell, characterized by ionic dehydration, shrinkage in the ion-water bond length and formation of cation-anion pairs, whereas the Cu^{2+} ions retain their bulk-like local structure till being driven to bond directly to the solid surface. Interestingly, a complete $Cu^{2+} \rightarrow Cu^{1+}$ reduction was realized at the end of further dehydration via thermal vacuum treatment at 110°C, which can be reversed at room temperature only when the filling fraction is above 14% and the interfacial water is definitely thicker than one monolayer. The underlying mechanism will be discussed.

II. EXPERIMENTAL

A. Sample Preparation

Disks ($\phi 7 \times 1.5$ mm) of Vycor® 7930 glass with mesopores of 7.6 nm in diameter, the specific inner surface area amounting to 122.5 m^2/g, were used in this experiment. The large pore size

excludes the confinement effect, thus helps focus on the effect of interfacial water. In order to completely remove the organic pollutants inside the pores, the glass disks were pretreated strictly following the procedure described in Ref. 19.

Bulk aqueous solutions of $CuBr_2$ were obtained by dissolving an appropriate amount of $CuBr_2$ salt (Sigma, 99.99 wt.%) into de-ionized water. For the 0.1 M solution of $CuBr_2$ here concerned, its pH value is 4.0, thus it does not require any pH-value adjustment to refrain Cu^{2+} ions from attaching to the glass surface. This assertion holds equally for the reference sample of 1.0 M, of which the pH value is 2.3. To fully load the mesopores with pure water or solution, the container holding the water or solution, with the glass disks immersed therein, was shaken vigorously for 8 h. Tissue paper was used later to remove the water or solution outside the mesopores via absorption. Inductively coupled plasma atomic emission spectroscopy was applied to determine the amount of Cu^{2+} ions inside the pores by comparing the Cu:Si ratio for the desiccated samples, which confirmed that the solution confined in the mesopores maintains the bulk concentration.

The loaded samples were subjected to the desorption/adsorption cycle of water without altering the amount of Cu^{2+} and Br^{1-} ions, and investigated in the different intermediate stages. Water content in the pores was adjusted through controlling the environmental humidity which was maintained by a mixture of high-purity N_2 (99.999%) and N_2 saturated with water vapor at proper flux ratios.[20] The desorption of water proceeds in two steps, i.e., following the desorption at room temperature in pure nitrogen, by which the filling fraction would be stabilized at ∼9%, the sample was further thermally treated in vacuo (10^{-4} Pa) at 110°C for ∼12 h to remove the residual water. This thermal vacuum treatment procedure can bring the filling fraction down to 5% (corresponding to a water layer less than one monolayer. The first monolayer corresponds to a filling fraction of ∼7.6%, see supplemental material[35]), and by the time of making the next XAS analysis it rises again to ∼6% due to water adsorption from the ambient, which constitutes the starting point for the subsequent adsorption process. Adsorption of water to a desired filling fraction can be simply realized by exposing the thermally treated samples to the mixture of nitrogen and water vapor at room temperature. After the adsorption or desorption equilibrium had been achieved, the samples were immediately sealed in a cell covered with a 2-μm thick Mylar film for subsequent test. For clarity and brevity, 'de' and 'ad' will be used in the article as subscript to the denotation of filling fraction, ϕ, or put before the value of the filling fraction, to specify whether the filling fraction refers to a sample at the end of a desorption process or an adsorption process. Since the ion concentration in a sample previously loaded with 0.1 M solution and now at $\phi = 10\%$ corresponds to that in the 1.0 M bulk solution, samples filled with 1.0 M bulk solution were also investigated as reference.

B. XAS Analysis

XAS spectra were measured near the Cu and Br *K*-edges in fluorescence mode at Beijing Synchrotron Radiation Facility on the 1W1B beamline and at Shanghai Synchrotron Radiation Facility on the BL14W1 beamline. A non-dispersive Si(111) double-crystal monochromator was used to focus the light beam. High-order harmonic rejection was realized by detuning the monochromator such that the maximum transmitted beam flux was reduced by 30-50%. Energy calibration was done by assigning the first inflection point of the absorption edge to 8980.3 eV for Cu and to 12658 eV for Se. In addition, the *K*-edge XAS spectra for $Cu^{2+}$and Br^{1-} ions in bulk $CuBr_2$ solutions and in three crystalline reference compounds, i.e., $CuBr_2$, CuO, and $Cu(OH)_2$, were also collected in transmission mode for comparison. EXAFS spectra were fitted using the R-space XAS analysis code FEFFIT[21] (for details, see supplemental material[35]).

III. RESULTS AND DISCUSSION

It is well-known that for Cu^{2+} ions in solution held in Vycor glass, direct bonding to the glass surface can hardly occur at pH values up to 4.0, even though the point of zero charge for SiO_2 is pH=2.0.[6] Therefore, for all the situations involved in the current work, the glass surface can be taken as neutral, and the Cu^{2+} and Br^{1-} ions in the fully-loaded mesopores reside in water.

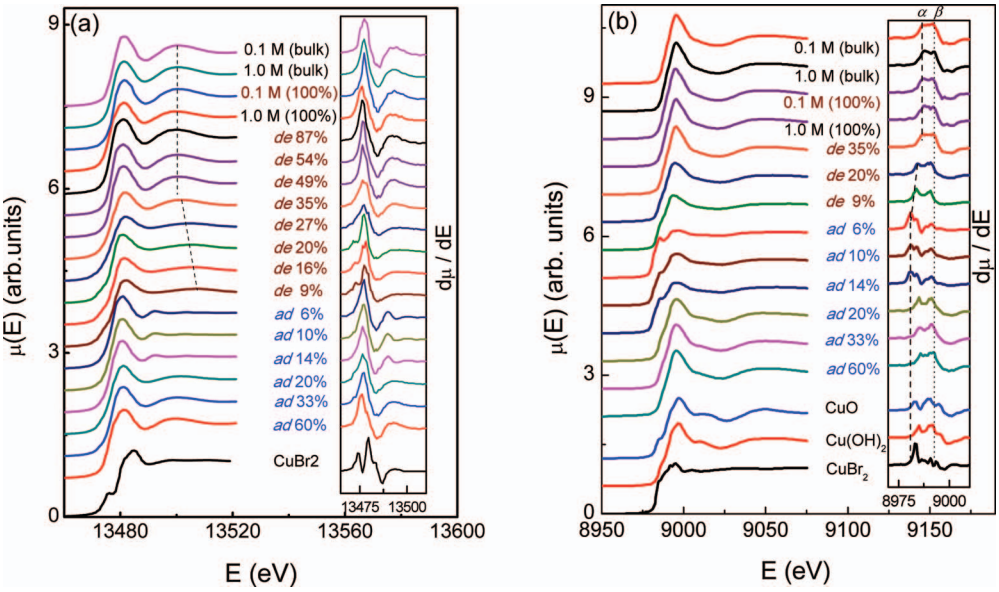

FIG. 1. Variation of Br *K*-edge (a) and Cu *K*-edge (b) XANES spectra obtained in a desorption-adsorption cycle for the 0.1 M $CuBr_2$ solution confined in Vycor mesopores. The insets show the corresponding first derivatives to enhance the features of variation, and dashed lines are added to guide the eye. Also curves for 0.1 and 1.0 M bulk solutions are presented for comparison. For the Cu K-edge, XANES curves obtained on crystalline $CuBr_2$, $Cu(OH)_2$ and CuO samples are also presented as reference.

To drive the hydrated ions into the interfacial region and to bring them back to the core water, the adsorption/desorption cycle of water was performed. By desorption of water to the point of capillary decondensation, only interfacial water persists. Further desorption proceeds via the continuous thinning of the interfacial water layer. As shown in Figure S1, a dilute salt solution does not alter the adsorption/desorption isotherms of water in mesopores. Due to the increased self energy of hydrated ions when approaching the surface (the dielectric constant decreases with the desorption of interfacial water. It is as low as 2-10 for the first monolayer of adsorbed water[2]), ions confined in the interfacial water layer still prefer staying far away from the pore surface. This is to say that the distance between the hydrated ions and the pore surface can be adjusted by carefully controlling the desorption process of interfacial water. The closer to the surface, the stronger the influence of hydrogen bonding interaction between water molecules and the confining surface on the hydration structure of ions.

Filling fraction-dependent XANES spectra, μ(E), for Br *K*-edge and Cu *K*-edge are presented in Figures 1 and 2, and the related EXAFS spectra ($k^2\chi(k)$) as well as the corresponding Fourier transformations (FT[$k^2\chi(k)$]) are displayed in Figure 3. Also spectral profiles for crystalline $CuBr_2$, $Cu(OH)_2$, and CuO are included as reference. With the filling fraction decreased to $\phi_{de} = 35\%$ which corresponds to a water layer ~1.05 nm in thickness (for details about the estimation of water layer thickness, see supplemental material[35]), no obvious influence on the coordination structure of the ions can be identified—both the XANES spectra in Figure 1 and the EXAFS spectra in Figure 3 remain quite the same as those of the bulk solution. This observation suggests that until this point the hydrated Br^{1-} and Cu^{2+} ions in the mesopores adopt a concentration-independent coordination structure, as in the bulk solution of concentrations ranging from 0.1 M to 1.0 M (see Tables S1 and S2 in supplemental material[35]). This assertion is also valid for the adsorption process when $\phi_{ad} \geq 35\%$. The reason lies in the fact that it is at $\phi_{de} = 35\%$ that the capillary decondensation of mesopores comes to the end (see the adsorption-desorption isotherm in Figure S1 in supplemental material[35]), which means that for $\phi > 35\%$, water in the pores exists as both interfacial water and core-water. Clearly, only when the hydrated ions stay in the core water can they maintain their bulk-like coordination structure. This is to say that so long as there is core water, the hydrated Cu^{2+} and Br^{1-} ions prefer staying therein, keeping away from the interfacial water.

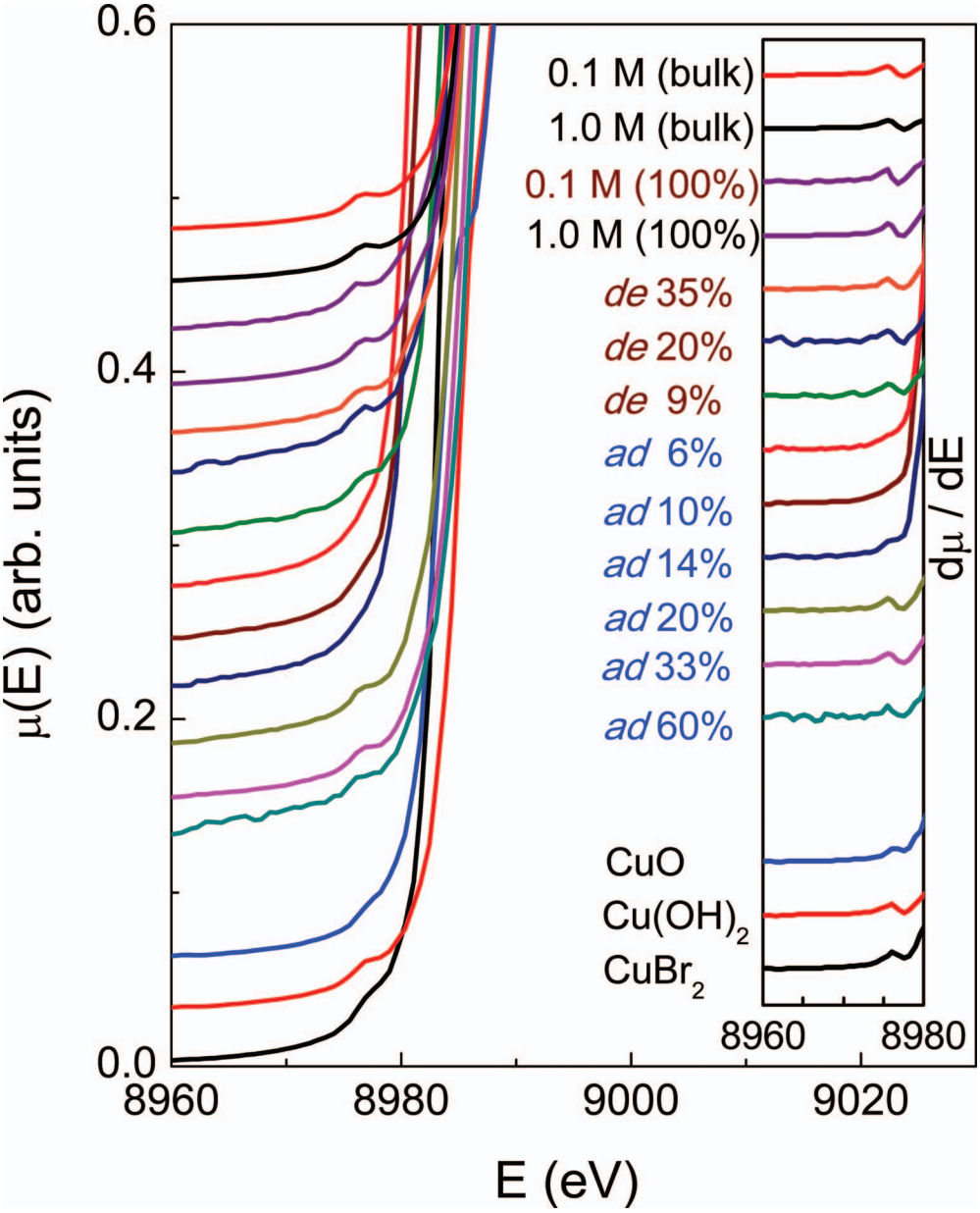

FIG. 2. Local magnification of the rising slope on the Cu *K*-edge XANES profiles in fig. 1(b) in the energy range between 8960 and 8985 eV.

When the filling fraction falls below 35%, noticeable changes first appear in the Br *K*-edge spectral profiles (μ(E), dμ/dE and $k^2\chi(k)$), as can be easily recognized from a peak on the μ(E) curves—marked by a dashed line in Figure 1(a) —which shifts steadily toward higher energy with the decreasing filling fraction, and from the shadowed region on $k^2\chi(k)$ curves in Figure 3(a). This points to a reduced Br-O bond length according to the Natoli rule,[22] as it is well accepted that the low-k region ($k < 3.5$ Å^{-1}) of $k^2\chi(k)$ spectra for Br *K*-edge comes mainly from the surrounding oxygen atoms. This claim was later confirmed by fitting the $k^2\chi(k)$ spectra in Figures 3(a) and 3(b), and the calculated coordination number, *N,* and bond length, *R,* are plotted in Figure 4 as a function of filling fraction (for details, see Table S1 in supplemental material[35]). We see that $R_{\text{Br-O}}$ decreases from 3.33 Å at $\phi_{\text{de}} = 35\%$ to 3.21 Å at $\phi_{\text{de}} = 9\%$, a remarkable shrinkage by 0.12 Å. At the same time, $N_{\text{Br-O}}$ decreases from 5.1 to 2.5. In addition, accompanying the collapse of the coordination

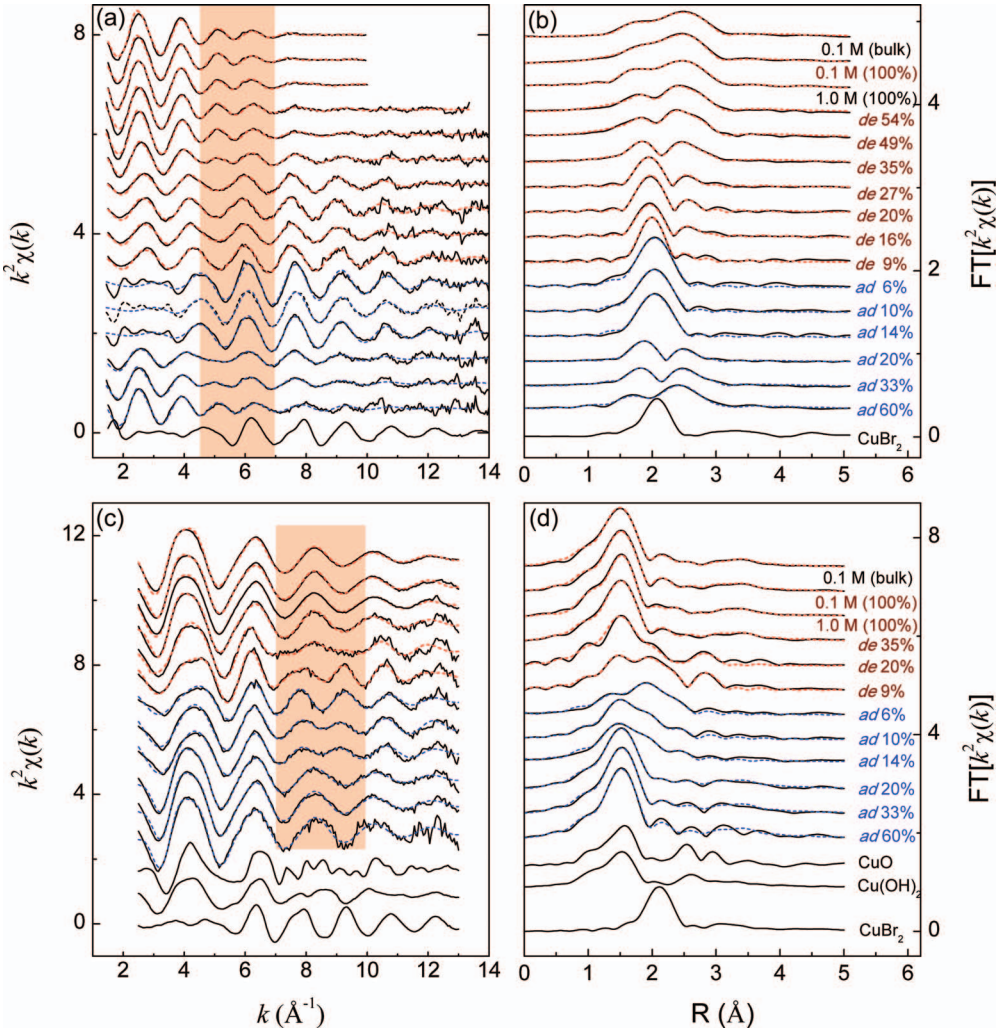

FIG. 3. Filling fraction-dependent *K*-edge EXAFS spectra and their corresponding Fourier transformations for hydrated Br^{1-} (a-b) and Cu^{2+} (or Cu^{+}) (c-d) ions, respectively. The results for 0.1 M bulk solution, and for samples fully-filled with 0.1 M and 1.0 M solutions, are presented for comparison. The shadowed zones are to guide the eye, wherein the transmutation of the peak profile in the desorption-adsorption cycle can be identified.

shell of the partially dehydrated Br^{1-}, a small amount of Cu-Br ion pairs emerge within the range $35\% \geq \phi_{de} \geq 20\%$ (Figure 4(b)). As mentioned above, for $\phi_{de} < 35\%$, the water in mesopores only exists as interfacial water, thus all the observed changes here correspond to the restructuring of the first coordination shell of Br^{1-} ions to fit the surrounding interfacial water. This observation is in contrary to the situation in supercritical water where, following the dehydration of Br^{1-} ions, $R_{Br\text{-}O}$ always becomes larger.[23] Such details about the behavior of ions entering the interfacial water are unlikely to be revealed by dielectric constant measurement.

Unlike Br^{1-} ions, the coordination structure of Cu^{2+} ions begins to change only when $\phi_{de} = 20\%$ (the corresponding water layer thickness is ~0.7 nm), see Figures 1(b) and 3(b). The different filling fraction-dependence of coordination structure for hydrated Cu^{2+} and Br^{1-} ions can be attributed to the large difference in their hydration energies, as $\Delta H_{hydr}(Cu^{2+}) = -2105$kJ/mol while $\Delta H_{hydr}(Br^{1-}) = -345$kJ/mol at 298.15 K.[24] The higher hydration energy helps the Cu^{2+} ions to maintain a bulk-like coordination shell even after having entered the interfacial water. At $\phi_{de} = 20\%$, a peak emerges on the Fourier-transformed EXAFS spectrum (without phase shift correction) around $R = 2.8$ Å (Figure 3(d)). This peak could be fitted by considering the Cu-Si, Cu-Cu, and Cu-(Si+Cu) paths,

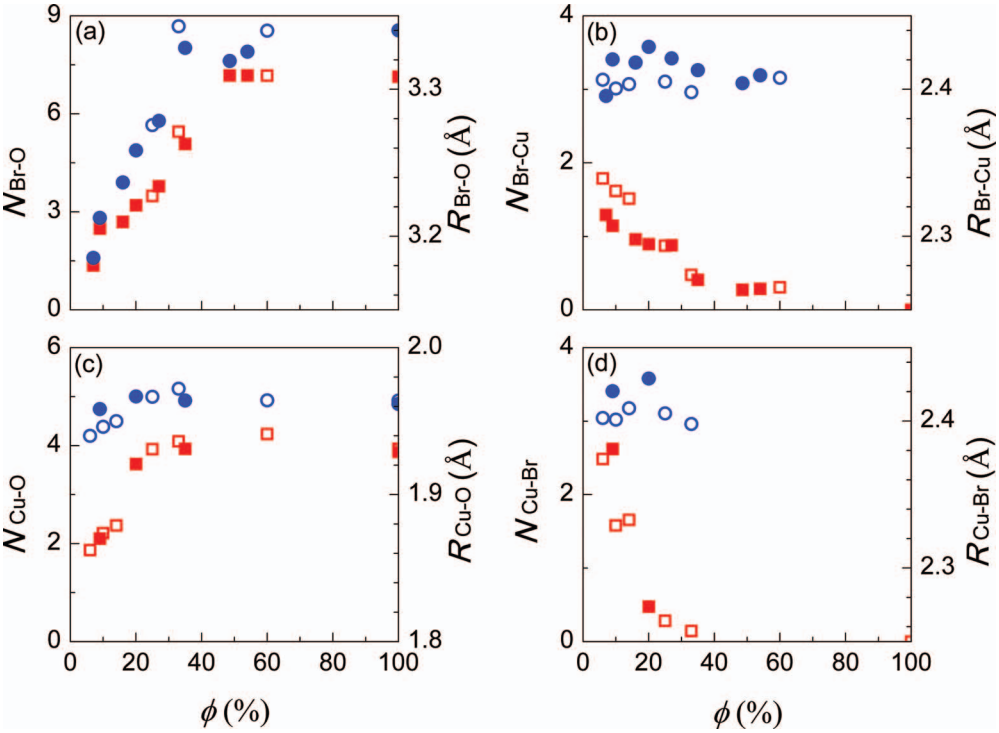

FIG. 4. Filling fraction dependence of coordination number (square) and bond length (circle) for Cu^{2+} (or Cu^{+}) and Br^{1-} ions in the two-step desorption process (solid symbols) and the adsorption process (hollow symbols).

and the result leads to a coordination shell of Cu-(1.0Si+1.5Cu), with $R_{Cu\text{-}Si} = 3.15$ Å, and $R_{Cu\text{-}Cu} = 3.12$ Å (for details, see Figure S4 and Table S3 in supplemental material[35]). The appearance of Cu-Si bonds indicates that the hydrated Cu^{2+} ions are now directly attached to the pore surface, and $R_{Cu\text{-}Si} = 3.15$ Å (with phase shift correction) together with $N_{Cu\text{-}Si} = 1$ support the view that monodentate binding of Cu^{2+} ion to the SiO_4 tetrahedron is more favorable.[25] Now, a fact becomes clear: Cu^{2+} ions will retain their bulk-like coordination structure until inner-sphere complexes are formed.

Starting at $\phi_{de} = 20\%$, the peak accentuated by the dashed line α on the $d\mu/dE$ curve for Cu *K*-edge (Figure 1(b)) shifts steadily towards lower energy. The position of this peak can be taken as E_0 for the absorption edge. Usually, a decrease in E_0 is caused by either or both of the following two factors: reduction of the transition metal ions, here Cu^{2+} ions, or change in their coordination structure. The latter point has been illustrated by the XANES spectra of several reference compounds of copper, see Figure 1(b). Whether the reduction process $Cu^{2+} \rightarrow Cu^{1+}$ has occurred or not can be judged by the absence or presence of the pre-edge transition peak at approximately 8976.8 eV (Figure 2), which arises from the $1s \rightarrow 3d$ transition of the Cu^{2+} ion. For a Cu^{1+} ion, the $1s \rightarrow 3d$ transition is forbidden since it has a closed *d* shell. Within the range of $100\% \geq \phi_{de} \geq 9\%$, this $1s \rightarrow 3d$ transition peak always appears and has similar intensities (Figure 2), therefore the possibility that the Cu^{2+} ions have been to some extent reduced by far can be excluded. On the basis of curve-fitting for the Fourier-transformed spectra (Figure 3(b)), obvious change in the first coordination shell of Cu^{2+} ions was confirmed when the filling fraction falls below 20%, i.e., $N_{Cu\text{-}O} = 3.6$ and $N_{Cu\text{-}Br} = 0.5$ at $\phi_{de} = 20\%$, while $N_{Cu\text{-}O} = 2.1$ and $N_{Cu\text{-}Br} = 2.6$ at $\phi_{de} = 9\%$. This is to say that at $\phi_{de} = 9\%$, each Cu^{2+} ion is coordinated in average with approximately 2.6 Br^{1-} ions in the first shell and 1.5 Cu^{2+} ions in the second shell. A fact should be pointed out that the ratio of water molecules to Cu^{2+} ions in the pores is still 55:1 even at $\phi_{de} = 9\%$. In contrary to the large change in the first coordination shell, the second coordination shell of Cu^{2+} ions remains almost unaltered in this region. The only detectable change was for σ^2_{Cu-Cu} which decreases from 1.49×10^{-2} to 6.3×10^{-3} Å^2, implying probably a more stable second coordination shell.

On the Cu *K*-edge XANES spectra for the sample experienced thermal vacuum treatment at 110°C, of which the filling fraction has reassumed a value of ∼ 6% at the moment of spectral measurement from $\phi_{de} \sim 5\%$ at the end of thermal vacuum treatment, the $1s \rightarrow 3d$ transition peak at 8976.8 eV is still absent. This peak reappears on the curves for $\phi_{ad} \geq 20\%$ (Figure 2). For $\phi_{ad} \leq 14\%$, $E_0 = 8981.2$ eV (see Figure 1(b)), and this low energy edge-position for XANES spectra can be attributed to the $1s \rightarrow 4p$ transition of the Cu^{1+} species.[26] These two observations support the conclusion that $Cu^{2+} \rightarrow Cu^{1+}$ reduction occurs in the process of thermal vacuum treatment, with the filling fraction being somewhere between 9% and 5%. At the same time, that $N_{Cu\text{-}O}$=2.1, $N_{Cu\text{-}Br}$=2.6 at $\phi_{de} = 9\%$ and $N_{Cu\text{-}O}$=1.9, $N_{Cu\text{-}Br}$=2.5 at $\phi_{ad} = 6\%$ (see Figure 4 and Table S2 in supplemental material)[35] also suggests that the coordination structure of the first coordination shell for copper ions suffers only a negligible influence from the reduction transition. Noticeable change in the coordination structure can be seen in the second shell, where the original peak at ∼2.8 Å only retains one third of its intensity after the reduction process (Figure 3(d)). There are two reasons responsible for this weakening of peak intensity: reduced coordination number and increased Debye-Waller factor σ^2. It should be pointed out that the change in the Debye-Waller factor suffices not to explain such a large decrease in peak intensity, therefore one can conclude that the coordination number of the second shell has become less during the $Cu^{2+} \rightarrow Cu^{1+}$ reduction transition.

At $\phi_{ad} = 20\%$, the $1s \rightarrow 3d$ transition peak recovers, at the same time it reassumes the intensity at $\phi_{de} = 9\%$ (Figure 2). In addition, E_0 also rises to 8985.2 eV. These two features strongly suggest that oxidation of Cu^{1+} to Cu^{2+} takes place near $\phi_{ad} = 20\%$ which corresponds to a water layer of ∼0.7 nm in thickness. Accompanying this oxidation process, obvious change in the coordination structure was detected, $N_{Cu\text{-}O}$=2.4 and $N_{Cu\text{-}Br}$=1.7 at $\phi_{ad} = 14\%$, while $N_{Cu\text{-}O}$=3.9 and $N_{Cu\text{-}Br}$=0.3 at $\phi_{ad} = 20\%$, see Figure 4.

For $\phi_{ad} \leq 14\%$, hardly any Br-O bonds could be detected. At $\phi_{ad} = 20\%$, the Br-(H-O) path becomes pronounced, and Br-O bonding suddenly emerges with $N_{Br\text{-}O} = 3.5$, and $N_{Br\text{-}Cu} = 0.9$. For comparison, notice that $N_{Br\text{-}Cu}$=1.5 at $\phi_{ad} = 14\%$. This indicates that accompanying the $Cu^{1+} \rightarrow Cu^{2+}$ transition, hydration of Br^{1-} ions occurs abruptly. With $\phi_{ad} > 20\%$, the first shell of Cu^{2+} ions is insensitive to the filling fraction. However, the coordination shell of Br^{1-} ions keeps changing till $\phi_{ad} = 35\%$, when capillary condensation takes place and the ions drift again into core water.

So far, two important conclusions can be drawn. First, the rehydration process of cations and anions here occurs only when sufficient water is available in the mesopores. Second, the reoxidation process of Cu^{1+} to Cu^{2+} is accompanied by an abrupt hydration of copper and bromine ions within the range of $14\% < \phi_{ad} < 20\%$, when the interfacial water is definitely thicker than one monolayer. As to the correlation between hydration and oxidation, it calls for further studies.

The energy barrier a hydrated ion confronts when it passes through the interfacial water layer is an important factor in determining many essential processes concerning ionic adsorption, permeation, etc. When the mesopores are only partially filled, each filling fraction may define a different condition for the water therein. As shown in Figure S1, the addition of a small amount of salt does not alter the adsorption/desorption isotherm of water in Vycor mesopores (0.1 M $CuBr_2$ corresponds to a copper ion density of ∼0.1/nm^2 when attached to the inner surface of the mesopores). This salt content-independent desorption-adsorption isotherm suggests that the previously discussed adsorption and desorption models of water in Vycor glass, formulated on the basis of dielectric constant measurement and liquid-solid transition investigation, are still valid.[20,27] Particularly, water desorption in Vycor mesopores comprises of capillary decondensation and thinning of interfacial water film. As mentioned above, the first coordination shell of both cations and anions remains quite the same as in bulk solution until $\phi_{de} = 35\%$ when core water is no more available, it then becomes strongly sensitive to the filling condition. Therefore, it can be concluded that the coordination structure variation of ions here results entirely from the interfacial water rather than the size effect of mesopores. With decreasing filling fraction below $\phi_{de} = 35\%$, the interfacial water layer becomes more and more closer to the pore surface, and the dielectric constant of interfacial water also decreases continuously.[2] At the same time, more and more water molecules are stripped away from the first shell of Br^{1-} ions, and Cu-Br ion pairs emerge and multiply. According to our experimental results, hardly any Cu-Br ion pairs can be detected in the $CuBr_2$ bulk solutions up to 1.0 M. This observation is consistent with a recent measurement on $CuBr_2$ bulk solution in the concentration

range from 0.1 M to 0.5 M,[28] but opposite to the speculation that half of the Cu^{2+} and Br^{1-} ions have already paired even at concentrations < 0.5 M.[29,30]

The thermal reduction process $Cu^{2+} \rightarrow Cu^{1+}$, taking place at somewhere between $5\% < \phi_{de} < 9\%$, is already effected at 110°C. The cation-anion pair has been taken as one of the most important reasons for the large difference in thermal-reduction temperatures for Cu/Vycor and Cu/ZSM-5 zeolite. In the latter case the cation-anion pair is absent,[31–34] and $Cu^{2+} \rightarrow Cu^{1+}$ reduction begins to be measurable at ∼300°C, and a complete reduction is achievable only at ∼500°C. Our finding may be helpful for the design of new catalysts to be used at low temperatures. In association with the reduction of Cu^{2+} ions, either the Br^{1-} ions or Si-O radicals at the surface are oxidized, with the former choice being more probable, but this cannot be confirmed with the current technique.

Unlike in supercritical water where $R_{Br\text{-}O}$ increases while $N_{Br\text{-}O}$ decreases following the dehydration of Br^{1-} ions,[23] here a decreasing $R_{Br\text{-}O}$ was detected with the thinning of interfacial water layer. This difference in behavior between the supercritical water and the interfacial water might shed special light on the effect of interfacial water on the local structure of hydrated Br^{1-} ions in hydrophilic Vycor mesopores. As to the Cu^{2+} ion, due to the higher hydration energy, it retains its bulk-like coordination structure until it has to bond directly to the pore surface. In order to further reveal the effect of hydration energy on the coordination structure variation of metal ions in interfacial water, RbBr solution ($\Delta H_{hydr}(Rb^+)$ =-299 kJ/mol, much less than that of Cu^{2+})[24] confined in Vycor mesopores is now under scrutiny following the procedure given here.

IV. CONCLUSIONS

In summary, coordination structure variation in the desorption/adsorption cycle for hydrated Cu^{2+} and Br^{1-} ions in 0.1 M $CuBr_2$ solution confined in the nearly-neutral, hydrophilic Vycor mesopores were studied using XAS analysis. Several important conclusions can be drawn: (1) Hydrated Cu^{2+} and Br^{1-} ions prefer staying in core water, and maintaining a bulk-like coordination structure so long as there is core water in the mesopores; (2) After capillary decondensation, dehydration of Br^{1-} ions begins first, and the bond length between Br^{1-} ion and the coordinated water molecules shrinks. Dehydration of Cu^{2+} ions, beginning at $\phi_{de} = 20\%$, is accompanied by a sudden emergence of ion pairs; (3) From $\phi_{de} = 20\%$ on, Cu^{2+} ions bind directly to the inner surface of Vycor mesopores. (4) Thermal reduction $Cu^{2+} \rightarrow Cu^{1+}$ is effected already at 110°C, and reoxidation at room temperature occurs at $\phi_{ad} = 20\%$ when most counterions in the first shell have been replaced by water molecules. These results might be inspirable for further researches on the coordination structure variation of hydrated ions under different conditions.

ACKNOWLEDGMENTS

This work was supported by the NSFC Grant Nos. 10874208 and 50971023, by the National Basic Research Program of China Grant Nos. 2010CB630705 and 2009CB930801, and by the Knowledge Innovation Project of Chinese Academy of Sciences on Water Science Research.

[1] A. Parsegian, Nature **221**, 844 (1969).
[2] G. E. Brown, Jr *et al.*, Chem. Rev. **99**, 77 (1999).
[3] O. Beckstein, K. Tai, and M. S. P. Sansom, J. Am. Chem. Soc. **126**, 14694 (2004).
[4] A. Miyazawa, Y. Fujiyoshi, and N. Unwin, Nature **423**, 949 (2003).
[5] T. Ohkubo, T. Konishi, Y. Hattori, H. Kanoh, T. Fujikawa, and K. Kaneko, J. Am. Chem. Soc. **124**, 11860 (2002).
[6] W. Stumm and J. J. Morgan, *Aquatic chemistry: Chemical equilibria and rates in natural waters*, 3rd edition, (Wiley-Interscience Publication, 1996), Chapter 9.
[7] C. Y. Park, P. A. Fenter, K. L. Nagy, and N. C. Sturchio, Phys. Rev. Lett. **97**, 016101 (2006).
[8] L. J. Criscenti and D. A. Sverjensky, Amer. J. Sci. **299**, 828 (1999).
[9] G. E. Brown, Jr and G. A. Parks, Inter. Geol. Rev. **43**, 963 (2001).
[10] G. Bunker, *Introduction to XAFS: A practical guide to X-ray absorption fine structure spectroscopy* (Cambridge University Press, 2010), pp 8-35.
[11] P. Lagarde, A. Fontaine, D. Raoux, A. Sadoc, and P. Migliardo, J. Chem. Phys. **72**, 3061 (1980).
[12] P. S. Salmon, G. W. Neilson, and J. E. Enderby, J. Phys. C: Solid State Phys. **21**, 1335 (1988).
[13] A. Pasquarello *et al.*, Science **291**, 856 (2001).

[14] M. Benfatto, P. D'Angelo, S. D. Longa, and N. V. Pavel, Phys. Rev. B **65**, 174205 (2002).
[15] P. R. Smirnov and V. N. Trostin, Russ. J. Gen. Chem. **79**, 1591 (2009).
[16] P. D'Angelo, A. Di Nola, A. Filipponi, N. V. Pavel, and D. Roccatano, J. Chem. Phys. **100**, 985 (1994).
[17] R. Beudert, H. Bertagnolli, and M. Zeller, J. Chem. Phys. **106**, 8841 (1997).
[18] P. D'Angelo, V. Migliorati, and L. Guidoni, Inorg. Chem. **49**, 4224 (2010).
[19] X. F. Huang, Q. Wang, X. X. Liu, S. H. Yang, C. X. Li, G. Sun, L. Q. Pan, and K. Q. Lu, J. Phys. Chem. C **113**, 18768 (2009).
[20] L. W. Wang, Q. Wang, C. X. Li, X. J. Niu, G. Sun, and K. Q. Lu, Phys. Rev. B **76**, 155437 (2007).
[21] M. Newville, B. Ravel, D. Haskel, J. J. Rehr, E. A. Stern, and Y. Yacoby, Phys. B **208&209**, 154 (1995).
[22] C. R. Natoli, in *EXAFS and Near Edge Structure*, edited by A. Bianconi *et al.* (Springer, New York, 1983) p 43.
[23] V. Simonet, Y. Calzavara, J. L. Hazemann, R. Argoud, O. Geaymond, and D. Raoux, J. Chem. Phys. **117**, 2771 (2002).
[24] Y. Marcus, *Ion salvation* (Wiley-Interscience Publication, 1985) pp 107-108.
[25] S. F. Cheah, G. E. Brown, Jr, and G. A. Parks, J. Colloid Interface Sci. **208**, 110 (1998).
[26] L. S. Kau, D. J. Spira-Solomon, J. E. Penner-Hahn, K. O. Hodgson, and E. I. Solomon, J. Am. Chem. Soc. **109**, 6433 (1987).
[27] X. X. Liu, Q. Wang, X. F. Huang, S. H. Yang, C. X. Li, X. J. Niu, Q. F. Shi, G. Sun, and K. Q. Lu, J. Phys. Chem. B **114**, 4145 (2010).
[28] M. J. Yu, W. S. Chu, X. Chen, and Z. Y. Wu, J. Phys: Conf. Series **190**, 012060 (2009).
[29] A. Fontaine, P. Lagarde, D. Raoux, M. P. Fontana, G. Maisano, P. Migliardo, and F. Wanderlingh, Phys. Rev. Lett. **41**, 504 (1978).
[30] P. Lagarde, A. Fontaine, D. Raoux, A. Sadoc, and P. Migliardo, J. Chem. Phys. **72**, 3061 (1980).
[31] M. Iwamoto, H. Yahiro, K. Tanda, N. Mizuno, Y. Mine, and S. Kagawa, J. Phys. Chem. **95**, 3727 (1991).
[32] G. T. Palomino, P. Fisicaro, S. Bordiga, A. Zecchina, E. Giamello, and C. Lamberit, J. Phys. Chem. B **104**, 4064 (2000).
[33] C. M. Chanquía, L. Andrini, J. D. Fernández, M. E. Crivello, F. G. Requejo, E. R. Herrero, and G. A. Eimer, J. Phys. Chem. C **114**, 12221 (2010).
[34] Y. Kuroda, Y. Yoshikawa, S. Konno, H. Hamano, H. Maeda, R. Kumashiro, and M. Nagao, J. Phys. Chem. **99**, 10621 (1995).
[35] See supplemental material at http://dx.doi.org/10.1063/1.4704545 for explanation of data treatment, estimation of water layer thickness, 3 tables showing the analysis results of EXAFS data, and 4 figures illustrating the adsorption-desorption isotherm, the virtual cluster of 550 water molecules plus 10 Cu^{2+} ions and 20 Br^{1-} ions, and EXAFS profiles.

Supplemental Material

Coordination variation of hydrated Cu^{2+}/Br^{1-} ions traversing the interfacial water in mesopores

Q. Wang,[1] X. F. Huang,[1,2] C. X. Li,[1] L Q. Pan,[2] Z. H. Wu,[3] T. D. Hu,[3] Z. Jiang,[4] Y. Y. Huang,[4] Z. X. Cao,[1*] G. Sun,[1] and K. Q. Lu[1]

[1]Institute of Physics, Chinese Academy of Sciences, Beijing 100190, China

[2]Department of Physics, University of Science and Technology Beijing, Beijing 100083, China

[3]Institute of High Energy Physics, Chinese Academy of Sciences, Beijing 100039, China

[4]Shanghai Institute of Applied Physics, Chinese Academy of Sciences, Shanghai 201204, China

Email: zxcao@iphy.ac.cn

[*] To whom correspondence should be addressed. E-mail: zxcao@iphy.ac.cn

1. **EXAFS Analysis**

EXAFS spectral profiles were fitted by using the R-space XAS analysis code FEFFIT on the basis of standard EXAFS formula given by[1]

$$\chi(k) = \frac{F(k)S_0^2 N}{kR^2}\exp(-2R/\lambda(k))\exp(-2k^2\sigma^2)\times\sin\left(2kR+\delta(k)-\frac{4}{3}k^3C_3\right) \qquad (1)$$

Where k is the wave vector which is related to the kinetic energy of photoelectron by $\mathrm{k} = \sqrt{2\mathrm{m_e}(\mathrm{E}-\mathrm{E}_0)/\hbar^2}$ (E_0 is the binding energy of the corresponding energy level), R, N and σ^2 represent the separation of the probed atom with its neighbors, coordination number, and Debye-Waller factor, respectively, S_0^2 is a many-body amplitude reduction factor, C_3 is the third cumulant which describes the skewness of the atomic distribution. The values for $F(k)$, $\delta(k)$ and $\lambda(k)$, which are the effective single-scattering amplitude, the total phase shift, and the mean-free-path, respectively, were taken from the FEFF9 calculation of crystalline $CuBr_2$ (for Cu-Br) and of a virtual cluster of 550 water molecules plus 10 Cu^{2+} ions and 20 Br^- ions (for Cu-O, Br-O, Br-H, Br-H-O paths). The virtual cluster (for details, see Figure S2) was at first constructed using the Amorphous Cell Module of Material Studio 5.0, and then optimized using the Forcite Modules with the COMPASS force field.[2] S_0^2 was set at 0.93 and 0.86 for Br and Cu ions, respectively. The parameter defining the muffin-tin radii overlap for the H atom was set to 0.8, as recommended in the FEFF9 documentation.[3]

XAS Modeling

Because of the d^9 electronic configuration, it is usually assumed that Jahn-Teller distortion occurs in the $[Cu(H_2O)_6]^{2+}$ complex.[4,5] According to this model, each Cu^{2+} ion is coordinated with four equatorial O atoms at a shorter distance and two axial O atoms at a slightly larger distance. Recently, based on neutron diffraction, XANES spectral analysis and first-principle molecular dynamics simulation, a square-pyramidal five-coordination in the first coordination shell of the hydrated Cu^{2+} ion was confirmed.[6,7]

EXAFS curve-fitting performed in this work indicates that in the 0.1 M bulk solution**,** each Cu^{2+} ion is coordinated by four water molecules (N_{Cu-O} = 4) with a bond length of R_{Cu-O}=1.95 Å (see Figure S3 (a)-(b) and Table S2). These structural factors are in good agreement with published data.[8] This is to say that the method applied for the EXAFS analysis reproduces the result for bulk $CuBr_2$ solution.[8] Besides the first coordination peak in the *R*-space, the high-*R* peak around 3.2 Å (without phase shift correction) was also well fitted by considering only the multiple-scattering of the first hydration shell (σ^2 values corresponding to each multiple-scattering path as proposed by Sakane *et al.* were adopted for the curve-fitting).[9] As well recognized, both the multiple-scattering of the first hydration shell and the single-scattering of the second hydration shell can lead to this high-*R* peak.[10-13] For hydrated Cu^{2+} ions, this high-*R* peak is largely caused by multiple-scattering of the first hydration shell.

In contrast to the strong electrostatic interaction between Cu^{2+} ions and water molecules, the weak interaction between Br^{1-} ions and the nearest water molecules results in a loose hydration shell around the Br^{1-} ion, noticing that $\Delta H_{hydr}(Cu^{2+})$ =-2100kJ/mol while $\Delta H_{hydr}(Br^{1-})$ =-330kJ/mol. Consequently, widely scattered $R_{Br\text{-}O}$ and $N_{Br\text{-}O}$ values have been reported depending on the probing methods and the theoretical models.[14] Here, contributions from both the single-scattering paths of Br-H and Br-O and the multiple-scattering paths of Br-H-O and Br-H-O-H were taken into account in the data fitting. We obtained $R_{Br\text{-}O}$ = 3.34Å, $N_{Br\text{-}O}$ = 7.1, and σ^2 = 0.030 for the 0.1M bulk solution (see Figure S3 (c)-(d) and Table S1), which agree well with the data obtained by other EXAFS measurements and by the Car-Parrinello molecular dynamics simulation.[14-16]

2. **Water Layer Thickness Estimation**

Filling fraction was determined by weighing the samples—100% filling of the mesopores (ϕ7.6 nm) corresponds to a specific mass augment of 0.25g/g. The thickness of the water layer was roughly estimated by considering each monolayer's contribution to the filling fraction. The amount of water in the first monolayer is determined by the density of hydroxyl on the inner surface of the glass. Supposing that each hydroxyl adsorbs one water molecule, and taking into account the fact that the density of hydroxyl for the mesoporous Vycor glass is ~4.9 / nm^2, [17] and the specific inner surface area is 122.5m^2/g, it can be calculated that the first monolayer makes a filling fraction of 7.2%. The second monolayer is assumed to be a hexagonal close-packing of water molecules which are taken as spheres of 0.35 nm in

diameter. [18] Thus this second monolayer contributes 12.4% to the filling fraction. Some people also treated the first monolayer this way,[19] and in this circumstance the first monolayer may correspond to a filling fraction of 13.6%. Similarly, the filling fraction arising from the third monolayer is estimated to be 11.2%. Hence, we come to the conclusion that a filling fraction of 35% roughly corresponds to three monolayers of water, and the thickness is $3 \times 0.35\,\text{nm}$, i.e., ~1.05 nm. The thickness values for other filling fractions were obtained by interpolation. Due to the irregularity of the pores and the inaccuracy of the model, the aforementioned calculation serves only a rough estimation. The true water layer is anticipated to be more compact. The estimated thicknesses in the current work can be understood as an upper limit for the interfacial water layer.

References

1. G. Bunker, Introduction to XAFS: A practical guide to X-ray absorption fine structure spectroscopy, Cambridge University Press (2010) p8-35.
2. Materials Studio 5.0, Accelrys Inc. San. Deigo, Ca, USA (AMORPHOUS_CELL Modules).
3. J. J. Rehr, J. J. Kas, M. P. Prange, A. P. Sorini, Y. Takimoto, and F. Vila, *Compt*. *Rend*. *Phys*. 10, 548 (2009).
4. P. Lagarde, A. Fontaine, D. Raoux, A. Sadoc, and P. Migliardo, *J*. *Chem*. *Phys*. 72, 3061(1980).
5. P. S. Salmon, G. W. Neilson, and J. E. Enderby, *J*. *Phys*. *C*: *Solid State Phys*. 21, 1335 (1988).
6. A. Pasquarello et al., *Science* 291, 856 (2001).

7. M. Benfatto, P.D'Angelo, S. D. Longa, and N. V.Pavel, *Phys. Rev. B* 65, 174205 (2002).
8. P. R. Smirnov, V. N. Trostin, *Russ. J. Gen. Chem.* 79, 1591 (2009).
9. H. Sakane, A. Muñoz-Páez, S. Díaz-Moreno, J. M. Martínez, R. R. Pappalardo, and E. S. Marcos, *J. Am. Chem. Soc*. 120, 10397(1998).
10. A. Muñoz-Páez, R. R. Pappalardo, and E. S. Marcos, *J. Am. Chem. Soc*. 117, 11710(1995).
11. P. D'Angelo, V. Barone, G. Chillemi, N. Sanna, W. Meyer-Klaucke, and N. V. Pavel, *J. Am. Chem. Soc*. 124, 1958(2002).
12. P. J. Merkling, A. Muñoz-Páez, and E. S. Marcos, *J. Am. Chem. Soc*. 124, 10911(2002).
13. P. D'Angelo, O. M. Roscioni, G. Chillemi, S. D. Longa, and M. Benfatto, *J. Am. Chem. Soc*. 128, 1853(2006).
14. P. D'Angelo, V. Migliorati, and L. Guidoni, *Inorg. Chem.* 49, 4224(2010) and references therein
15. P. D'Angelo, A. Di Nola, A. Filipponi, N. V. Pavel, D. Roccatano, *J. Chem. Phys*. 100 (1994).
16. R. Beudert, H. Bertagnolli, and M. Zeller, *J. Chem. Phys*. 106, 8841(1997).
17. L. T. Zhuravlev, *Langmuir* 3, 316 (1987).
18. E. Tombari, C. Ferrari, G. Salvetti, and G. P. Johari, *Thermochimica Acta* 492, 37 (2009).
19. J. Puibasset, and R. J. M. Pellenq, *J. Chem. Phys.* 122, 094704 (2005).

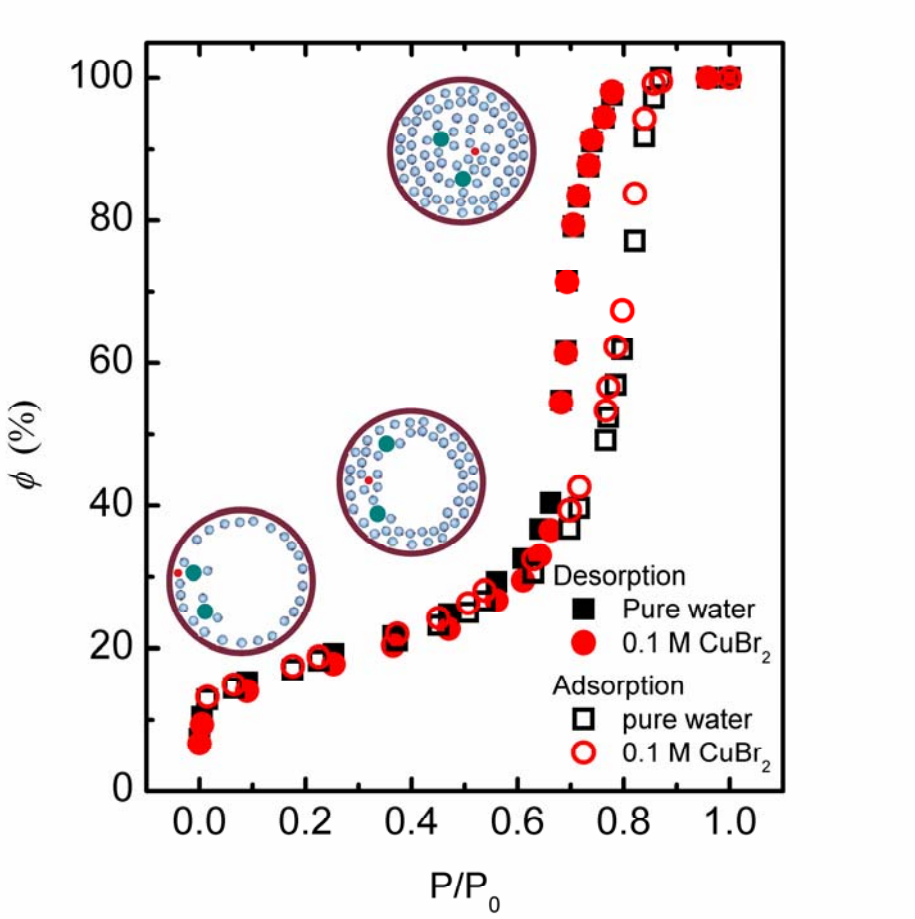

Figure S1. Desorption and adsorption isotherms for Vycor mesopores loaded with pure water (square) and 0.1 M $CuBr_2$ solution (circle), respectively. ϕ: filling fraction; P/P_0: relative humidity.

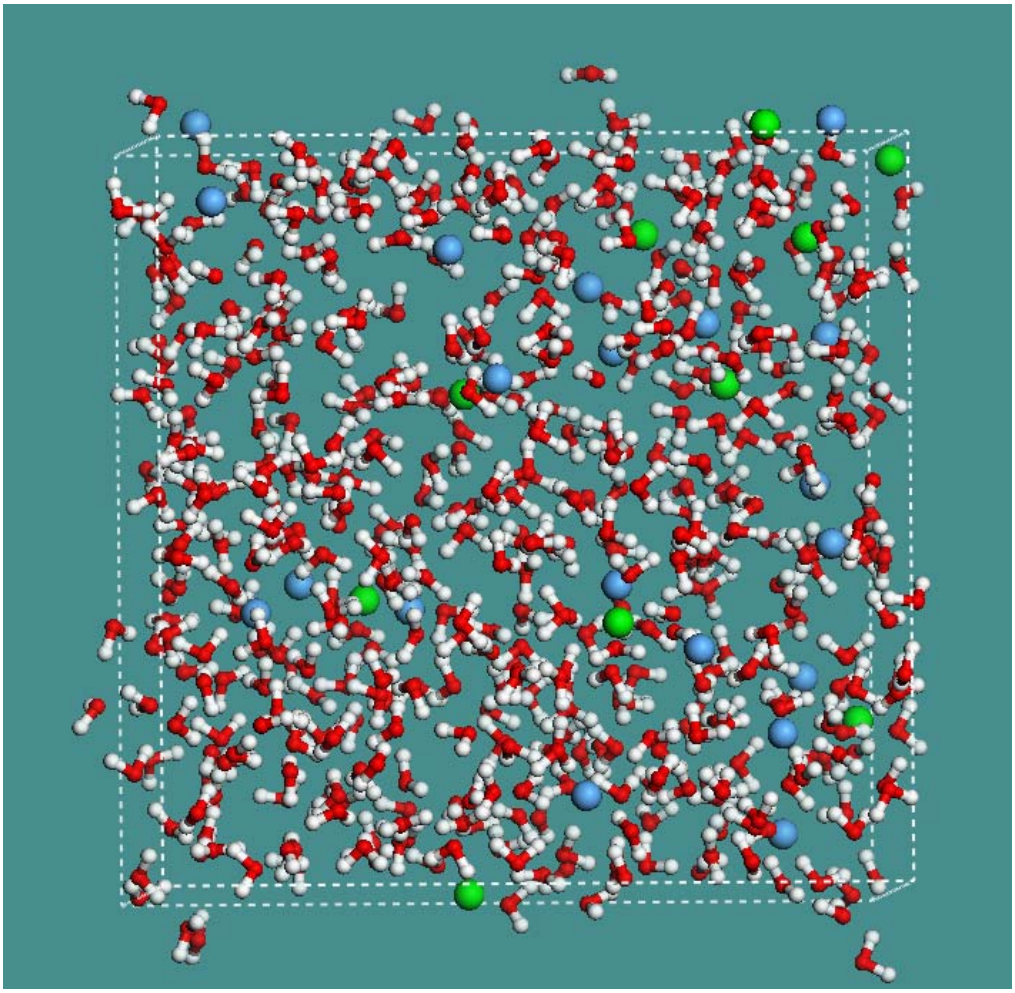

Figure S2. The virtual cluster of 550 water molecules plus 10 Cu^{2+} ions (green) and 20 Br^{1-} ions (blue).

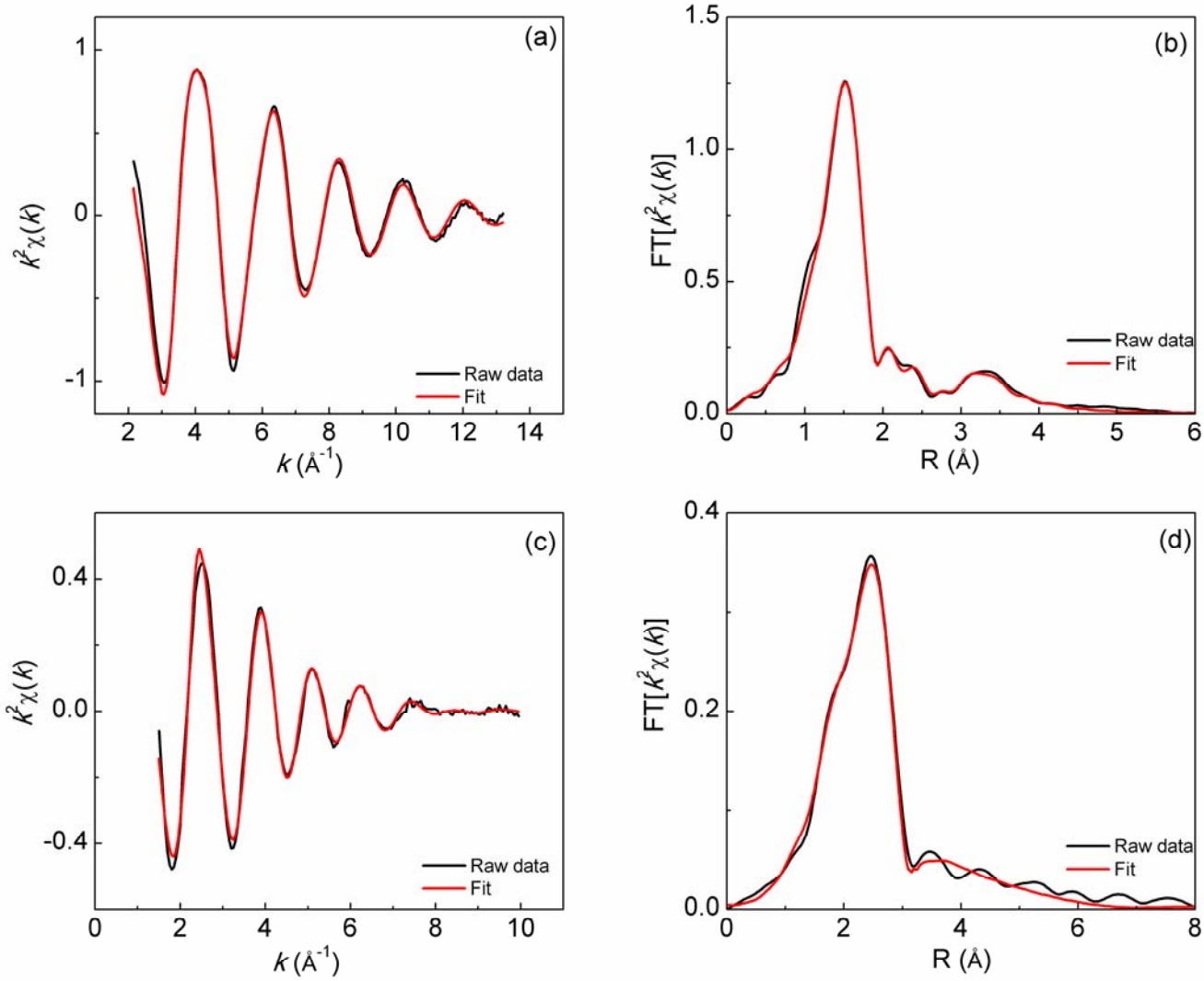

Figure S3. The EXAFS profile and the corresponding Fourier transform for Cu K-edge (a, b) and Br K-edge (c, d), respectively, measured in the 0.1 M $CuBr_2$ bulk solution.

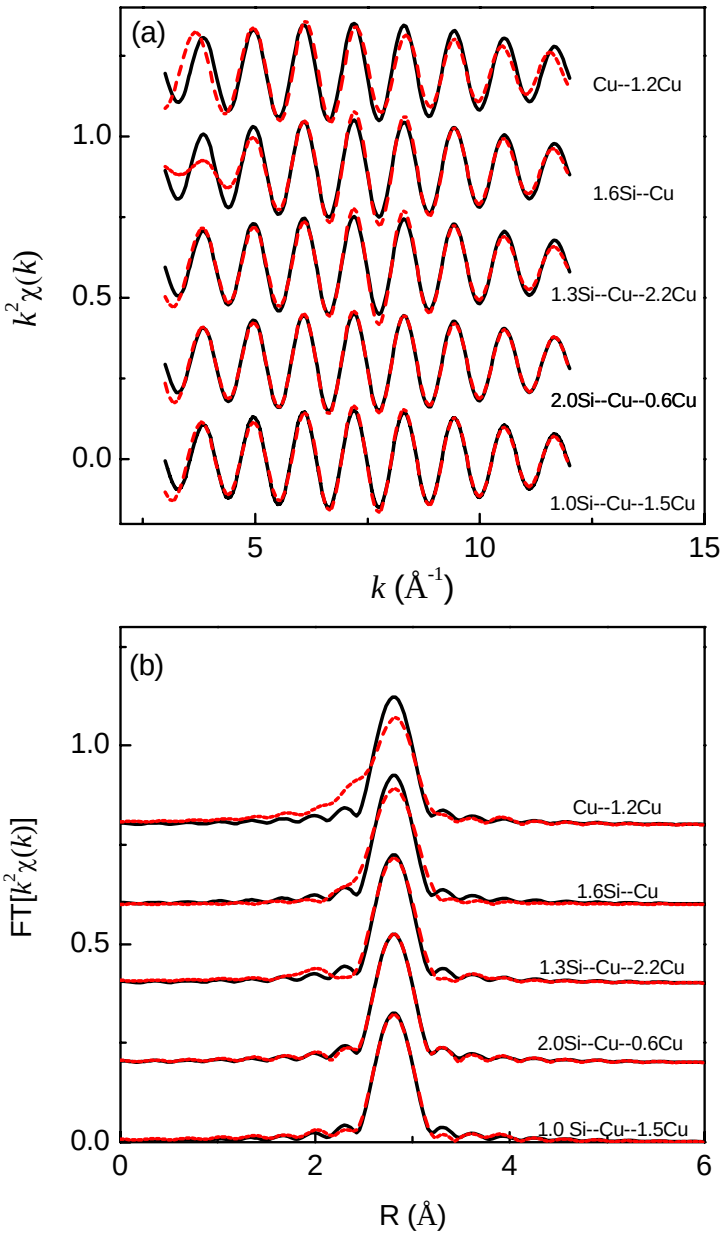

Figure S4. Raw experimental data of EXAFS for Cu *K*-edge measured in the sample with $\phi_{de} = 9\%$ (a) and the corresponding Fourier transformations (b). $3 < k < 12$Å^{-1}, and $1.5 < R < 4$ Å.

Table S1. Analysis results of EXAFS data for the Br *K*-edge

ϕ	Ab-Sc pair	*N*	*R*	σ^2	ΔE_0	C_3 ($\times 10^3$)	*R*-factor
0.1M bulk	Br-O	7.1	3.34	0.030	-1.8	0.8	0.021
0.1M 100%	Br-O	7.1	3.34	0.030	-1.8	0.8	0.021
1.0M 100%	Br-O	7.2	3.34	0.030	-1.7	1.0	0.022
deϕ=54%	Br-O	7.2	3.33	0.032	-1.3	-0.5	0.024
	Br-Cu	0.3	2.41	0.013	6.0		
deϕ=49%	Br-O	7.2	3.32	0.034	-1.3	-0.2	0.020
	Br-Cu	0.3	2.40	0.011	5.8		
deϕ=35%	Br-O	5.1	3.33	0.033	-0.5	1.2	0.027
	Br-Cu	0.4	2.41	0.010	-3.8		
deϕ=27%	Br-O	2.7	3.78	0.033	-0.6	2.5	0.020
	Br-Cu	0.9	2.42	0.009	-10		
deϕ=20%	Br-O	3.2	3.26	0.033	-1.5	4.2	0.028
	Br-Cu	0.9	2.43	0.007	-9.8		
deϕ=16%	Br-O	2.7	3.24	0.033	-1.9	1.8	0.020
	Br-Cu	1.0	2.44	0.0096	-8.53		
deϕ=9%	Br-O	2.5	3.21	0.033	-1.6	4.8	0.029
	Br-Cu	1.1	2.42	0.0076	-8.5		
ϕ_{ad} =6%	Br-Cu	1.8	2.41	0.0086	-5.8		0.023
ϕ_{ad} =10%	Br-Cu	1.6	2.40	0.0091	-6.6		0.025
ϕ_{ad} =14%	Br-Cu	1.5	2.40	0.0084	-7.2		0.019
ϕ_{ad} =20%	Br-O	3.5	3.28	0.033	-3.6	2.0	0.019
	Br-Cu	0.9	2.41	0.012	-9.4		
ϕ_{ad} =33%	Br-O	5.5	3.34	0.037	-1.6	0.9	0.024
	Br-Cu	0.5	2.40	0.010	-7.3		
ϕ_{ad} =60%	Br-O	7.2	3.34	0.037	-1.4	1.8	0.028
	Br-Cu	0.3	2.41	0.0090	3.8		

ϕ: filling fraction of mesopores; Ab-Sc: absorber-scatter; N: coordination number; R: distance (Å); σ^2: Debye-Waller factor (Å^2); ΔE_0: energy shift; C_3: anharmonic term of the O subshell; *R*-factor: goodness-of-fit parameter.

For the cases of ϕ_{ad} =6%, ϕ_{ad} =10%, and ϕ_{ad} =14%: $4 < k < 11.5$ Å^{-1}, $1 < R < 3$ Å.

For the bulk solution: $2 < k < 9$ Å^{-1}, $1 < R < 4$ Å.

For other samples: $2 < k < 11.5$ Å^{-1}, $1 < R < 4$ Å, and S_0^2=0.93.

Table S2. Analysis results of EXAFS data for the Cu *K*-edge.

ϕ	Ab-Sc pair	*N*	*R*	σ^2	ΔE_0	C_3 ($\times 10^4$)	*R*-factor
0.1M bulk	Cu-O	4.0	1.95	0.0054	-8.6	-0.7	0.0064
0.1M 100%	Cu-O	3.9	1.95	0.0054	-7.3	-1.7	0.0044
1.0M 100%	Cu-O	3.9	1.96	0.0051	8.8	0.9	0.0086
ϕ_{de}=35%	Cu-O	3.9	1.96	0.0051	8.8	0.9	0.0085
ϕ_{de} =20%	Cu-O	3.6	1.97	0.0078	-6.1	-0.2	0.0078
	Cu-Br	0.5	2.43	0.0046	-10		
ϕ_{de} =9%	Cu-O	2.1	1.96	0.0069	-3.7	1.5	0.0041
	Cu-Br	2.6	2.42	0.010	-8.2		
ϕ_{ad}=6%	Cu-O	1.9	1.94	0.013	-4.7	0.5	0.032
	Cu-Br	2.5	2.40	0.010	-6.9		
ϕ_{ad} =10%	Cu-O	2.2	1.95	0.0048	-4.2	-0.3	0.018
	Cu-Br	1.6	2.40	0.0083	-10		
ϕ_{ad} =14%	Cu-O	2.4	1.96	0.0065	-4.2	0.3	0.020
	Cu-Br	1.7	2.41	0.0099	-7.5		
ϕ_{ad} =20%	Cu-O	3.9	1.97	0.0063	-7.2	1.2	0.0085
	Cu-Br	0.3	2.41	0.0099	-8.1		
ϕ_{ad} =33%	Cu-O	4.0	1.97	0.0056	-6.9	1.7	0.0106
	Cu-Br	0.1	2.40	0.0098	9.3		
ϕ_{ad} =60%	Cu-O	4.2	1.96	0.0052	-7.8	0.7	0.0081

ϕ: filling fraction of mesopores; Ab-Sc: absorber-scatter; *N*: coordination number; *R*: distance (Å); σ^2: Debye-Waller factor (Å^2); ΔE_0: energy shift; C_3: anharmonic term of the O subshell; *R*-factor: goodness-of-fit parameter. $3 < k < 12$ Å^{-1}, $1 < R < 4$ Å, and S_0^2=0.86.

Table S3. Analysis results of the second coordination shell for the Cu *K*-edge EXAFS spectrum collected on the sample with ϕ_{de} = 9%.

Ab-Sc pair	*N*	*R*	σ^2	ΔE_0	*R*-factor
Cu--Cu	1.2	3.11	0.0069	-1.3	0.066
Cu--Si	1.6	3.27	0.0035	-7.3	0.134
Cu--Si	1.3	3.05	0.0058	-12.0	0.0208
Cu--Cu	2.2	3.08	0.0088	-7.7	
Cu--Si	2.0	3.39	0.0213	2.9	0.0036
Cu--Cu	0.6	3.10	0.0035	-4.0	
Cu--Si	1.0	3.15	0.0064	-8.4	0.0091
Cu--Cu	1.5	3.12	0.0063	-5.2	

Ab-Sc: absorber-scatter; *N*: coordination number; *R*: distance (Å); σ^2 : Debye-Waller factor (Å^2); ΔE_0: energy shift; *R*-factor : goodness-of-fit parameter. $3 < k < 12$ Å^{-1}, $1.5 < R < 4$ Å, and S_0^2=0.86. The introduction of the anharmonicity term C_3 did not improve the fitting result for the second shell of Cu^{2+} ions.